Lab on a Chip

COMMUNICATION

View Article Online
View Journal | View Issue

Cite this: *Lab Chip*, 2017, **17**, 640

Received 3rd December 2016,
Accepted 27th January 2017

DOI: 10.1039/c6lc01476c

rsc.li/loc

A 2.5-D glass micromodel for investigation of multi-phase flow in porous media†

Ke Xu,[a] Tianbo Liang,[a] Peixi Zhu,*[a] Pengpeng Qi,[a] Jun Lu,[b] Chun Huh[a] and Matthew Balhoff[a]

We developed a novel method for fabrication of glass micromodels with varying depth (2.5-D) with no additional complexity over the 2-D micromodels' fabrication. Compared to a 2-D micromodel, the 2.5-D micromodel can better represent the 3-D features of multi-phase flow in real porous media, as demonstrated in this paper with three different examples. Physically realistic capillary snap-off and the formation of isolated residual oil droplets were realized, which is not possible in 2-D micromodels. Droplet size variation during an emulsion flooding was investigated on the 2.5-D micromodel, showing that the droplet size decreases sharply at the inlet, with little change in size downstream of the micromodel. Displacement of light oil with ultra-low interfacial tension (IFT) surfactant was conducted in the 2.5-D micromodel, where we were able to visualize the generation and flowing of a microemulsion phase, which agrees with, and explains observations in experiments of more complex porous media.

Introduction

Flow, especially multi-phase flow, in porous media with micron-scale pores and throats has long been an important interest in many areas of science and engineering.[1] Oil–water separation processes,[2] waste water treatment,[3] transport of oil-soluble pollutants in soil and underground water,[4] and generation of foam and emulsion for chemical and food production,[5,6] are all important applications involving multi-phase flow. In hydrocarbon recovery from subsurface reservoirs, waterfloods,[7] conformance control[8,9] and enhanced oil recovery[10–14] are all multi-phase processes.

Investigation of multi-phase flow in realistic porous material samples, such as membrane devices and oil-displacement coreflood devices, is common.[15–17] In those studies, macro-scale data, such as pressure drop, outlet fluid properties, and saturation profiles, are often measured.[18,19] However, direct visualization and quantitative description of micron-scale behaviour of multi-phase fluids is still difficult, due to the complex 3-D geometry of real porous media (*e.g.* subsurface rocks).

Microfluidics provide a tool, which can be used to study and visualize multi-phase flow at the micron-scale, *i.e.* surrogates for pore bodies and throats. Recently, microfluidics have been used to study some fundamental flow phenomena in porous media including single phase flow of Newtonian[20] and non-Newtonian[21] fluids, multi-phase flow,[22–24] mechanisms of droplet formation[25–27]/coalescence,[28,29] and cross-interface mass-transport.[30] In addition, some single-channel geometries with varying cross-section size along the channel have been designed to study non-wetting phase trapping at pore-throat structures,[19] emulsion flow in parallel channels,[31] and other geometries relevant to enhanced oil recovery[32] and reservoir engineering[18] research.

Naturally-occurring 3-D porous media are complicated networks of pores and throats. While single-pore or single-channel flow studies are useful, they are not sufficient for fully understanding flow behaviour in porous media. Consequently, 2-D "micromodels", a simplified pore-throat network system on 2-D microchips, are often used to study flow in porous media. "2-D" here indicates the micromodel has varying size in horizontal dimensions but has uniform depth in the vertical dimension. In recent years, many common fluidic phenomena in porous media have been investigated by using 2-D micromodels, especially for enhanced oil recovery applications, such as particle retention,[9] water flooding,[7,33] foam flooding,[34,35] surfactant flooding,[36] and polymer flooding.[37]

These micromodels are limited by their 2-D geometry, *i.e.* their absence of varying depth. For example, in multi-phase flow "capillary snap-off"[38] is an important mechanism for oil and bubble break-up; it only occurs if the size of throats are smaller than that of pore bodies in the two dimensions perpendicular to the flow direction (the pressure at the "neck"

[a] *Department of Petroleum and Geosystems Engineering, The University of Texas at Austin, Austin, Texas 78712, USA. E-mail: zpeixi@utexas.edu*
[b] *McDougall School of Petroleum Engineering, University of Tulsa, Tulsa, OK 74104, USA*

† Electronic supplementary information (ESI) available. See DOI: 10.1039/c6lc01476c

must be larger than that of the droplet front). This limitation of micromodels is well documented and it has been noted[34] that "studying snap-off in 2-D porous media is inherently problematic". In addition, if pores are designed continuous (connecting with each other through throats) in a 2-D micromodel, the grains must be non-continuous (isolated from each other), while both grains and pores are continuous in natural-occurring 3-D porous media. This may have considerable significant effect on wetting-fluid imbibition. 3-D features in the micromodel geometry are therefore required for studying many physics in porous media, especially those related to multi-phase flow (*e.g.* two phase displacement, emulsion flow, foam flow, three-phase flow, *etc.*), where capillary effects are significant.

A few attempts have been made to fabricate microfluidic chips and even some micromodels with 3-D features in the geometry using 3-D printing.[39,40] Unfortunately, the resolution (tens of microns) and material limit (fusible) of current 3-D printing technology make it impossible to build a 3-D micromodel as a simplified model of realistic micron-scale porous media.[32,41]

In this communication, we introduce a novel and simple approach to fabricate "2.5-D" (depth-variable) micromodels, with no additional complexity in the fabrication procedure. The depth ratio of throat to pore body is easily controlled. We performed common multi-phase flow experiments on the 2.5-D micromodel, where we produced phenomena that has never been correctly observed (or were mistakenly presented) on a 2-D micromodel. We believe that 2.5-D micromodels could be a more advanced platform for a better understanding and optimization of current fluidic theories/models in porous media.

Fabrication and characterization of 2.5-D glass micromodels

Glass has long been used as a preferred material for microfluidic devices, because of its superior transparency, high hardness and ease to modify its surface wettability.[42,43] The most widely applied method to fabricate glass microfluidic chips follows a standard lithography process and hydrofluoric (HF) acid etching.[44] Horizontal dimensions of the microchannels are determined by the 2-D blueprint design (CAD), and the depth is obtained by HF-etching speed and time. The etched glass piece was bonded to a cover glass piece mostly by heating at 500–700 °C for hours. A sketch of the standard 2-D micromodel fabrication is shown in Fig. 1a.

Due to isotropic etching of HF, the cross-section of the channel is not strictly rectangular but somewhat trapezoidal. This is generally considered a disadvantage of HF etching because it makes the cross-section shape "non-ideal". In most previous 2-D micromodel studies, researchers either accepted the imperfection,[45] or attempted to avoid it by applying more complex/expensive technology, such as laser.[36]

Here we propose a novel approach that utilizes, rather than ignores or avoids, the isotropic HF etching and the resulting trapezoidal cross-section, followed by controlled fabrication of the micromodels with important 3-D features.

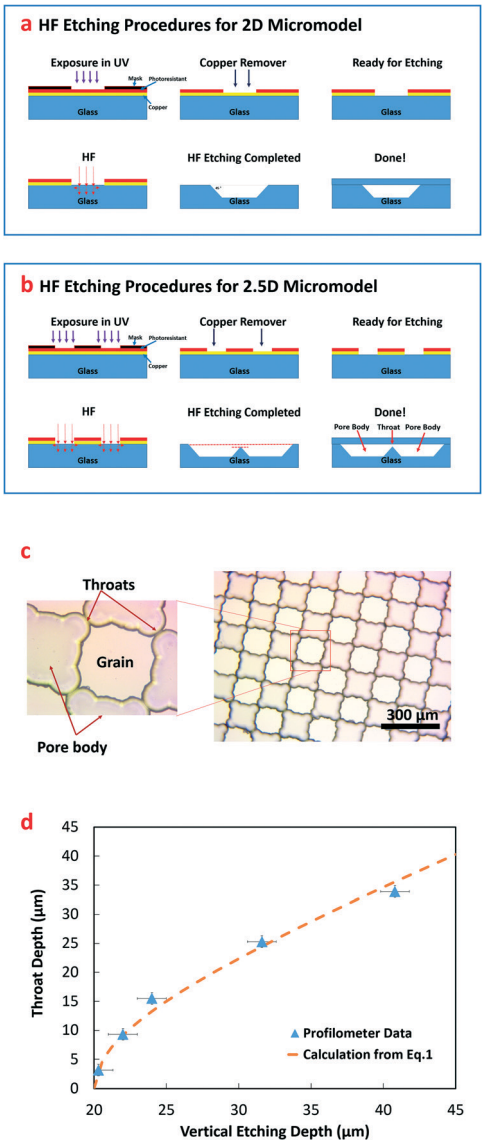

Fig. 1 a) Typical HF etching procedures to fabricate glass micromodel, where trapezoidal cross-section is formed due to the isotropic etching of HF. b) Fabrication of 2.5-D micromodel, where we obtain a shallower throat by making use of the isotropic etching of HF by controlling the distance between pores and the etching depth. c) Microscopic image of the 2.5-D micromodel. Grains, pore bodies, and barrier-like throats between neighbouring pore bodies. The formation of grains shape is illustrated in ESI.† d) Relationship between throat depth and vertical etching depth on the pore body. The blue triangles are data measured from profilometer, and the orange dot line is the data calculated from eqn (1).

As shown in Fig. 1b, if two neighbouring "pores" in the 2-D blueprint are designed close enough that the maximum horizontal etching distance (at the top) is larger than half of the minimum distance between two designed "pore edges", the glass wall between the two pores would form a "channel" at the upper side of pores after HF etching. Thus, we can create neighbouring pores connected by a throat, which is not

only horizontally narrower than the pore body (like previous 2-D micromodels), but also vertically shallower than the pore body. A microscopic image of a 2.5-D micromodel is shown in Fig. 1c. The micromodel consists of repeating pore-grain systems with every pore connected to four other pores. Noticeably, there is a barrier geometry (the throat) between two pore bodies where the depth is considerably smaller than the pore body.

Importantly, the depth difference between the pore body and the throat can be easily controlled by adjusting the maximum etching depth and the distance between pore bodies on the 2-D blueprint. A larger maximum etching depth can bring a smaller depth difference, while a larger distance between two pores on 2-D blue print can make the throat much shallower or even disappear. A theoretical equation is derived to predict the throat depth's (H_{throat}) relationship with maximum vertical etching depth (H_{pore}) and the minimum horizontal distance between the edges of two pores on the 2-D blueprint (L), as shown in eqn (1):

$$H_{throat} = \sqrt{H_{pore}{}^2 - \frac{1}{4}L^2} \quad (1)$$

Fig. 1d shows the plot between H_{pore} and the H_{throat}, when L is fixed at 40 μm, comparing data measured with a profilometer and that calculated by eqn (1). It shows that the data measured from the profilometer is predicted well by eqn (1) although with some minor positive bias.

Noticeably, according to eqn (1), as the throat size is only determined by neighbouring two pores on the blueprint, it is possible to create pores with unequal and anisotropic sizes and throats with different depths and widths, although we only demonstrate homogenous micromodels with isotropic pores in this work for simple validation. More discussion and illustration about the 3D structure is shown in ESI.†

Multi-phase flow experiments on 2.5 D glass micromodels

The 2.5-D micromodel can be used to study a broader range of physics than the 2-D model, especially those that involve capillary forces in multi-phase flow. We performed several experiments of multi-phase flow in a water-wet 2.5-D glass micromodel. From those experiments, some important phenomena were observed and analysed, the first using micromodels to our knowledge. Geometric parameters of the micromodel that we used for all the flow experiments shown in this paper are listed in Table 1.

Table 1 Geometric parameters of the 2.5-D glass micromodel applied in this paper

Geometric parameters	Length
Porous media length	2.4 cm
Total pore volume	7 μl
Pore body depth	20.3 μm
Throat width	23 μm
Throat depth	3.2 μm

Wetting phase imbibition

In water-wet hydrocarbon reservoirs (such as sandstone reservoirs) after oil phase is displaced by water (herein referred to as a waterflood), un-recovered oil is often classified by two types: residual oil, which is isolated oil droplets trapped by capillary forces in pore bodies, and unswept oil, which is oil that occupies a continuous region uninvaded by the water phase. If a reservoir is a relatively homogeneous porous medium, and if the oil is less viscous than the water phase, the residual oil (isolated oil droplets in pore bodies) is typically the majority of unrecovered oil.[46] This classic imbibition theory is presented by Dong *et al.*[47] and Muggeridge *et al.*,[10] as shown in Fig. 2a. In this section, waterflood experiments were performed on both a 2-D micromodel and a 2.5-D micromodel, with oil viscosity less than water.

The 2-D micromodel is identical in geometry to the 2.5-D micromodel (as listed in Table 1), except that the depth is uniformly 23 μm both at the pore bodies and at the throats. In both experiments, n-octane was used as the oil (non-wetting) phase and was pre-saturated into the micromodel before waterflood. Dyed water (coloured blue) was used as the aqueous (wetting) phase. The interfacial tension (IFT) between the two phases is 50.6 mN m^{-1}. Viscosity of water is 1.0 cP, and the viscosity of octane is 0.52 cP. In the experiment, the water flow rate was 7 μl h^{-1} (~2 ft per day along the porous medium).

Fig. 2b and c show the 2-D and 2.5-D micromodel after waterflood, respectively. It is clearly shown in the 2-D micromodel, a pore body is either occupied completely by water, or by continuous oil phase. No isolated oil droplet trapped in a pore body, as described in realistic porous media, was observed. The result is similar to previous 2-D micromodel observations on waterfloods from other researchers.[48,49] However, in the 2.5-D micromodel, almost every pore body traps an isolated oil droplet, with water phase occupying the throats and pore edges. It is exactly what the theory describes as shown in Fig. 2a, for realistic 3-D porous media. In summary, the formation of residual oil in real porous media matches our observation in 2.5-D micromodel well, but does not match the observation in 2-D micromodel. Thus, we claim that this 2.5-D model is more advanced in capturing and mimicking the multi-phase fluidic phenomena in 3-D porous media, than a traditional 2-D micromodel with uniform depth.

The transient process of water imbibition into the oil-saturated, water-wet 2.5-D micromodel is shown in Fig. 2d–g and Movie SA.† In the imbibition process, water phase did not displace the oil phase as a piston flow, but rather along pore body edges and the throats. Water's invasion along those high specific area region (throats and edges) was clearly induced by capillary force at the oil–water–glass contact line,

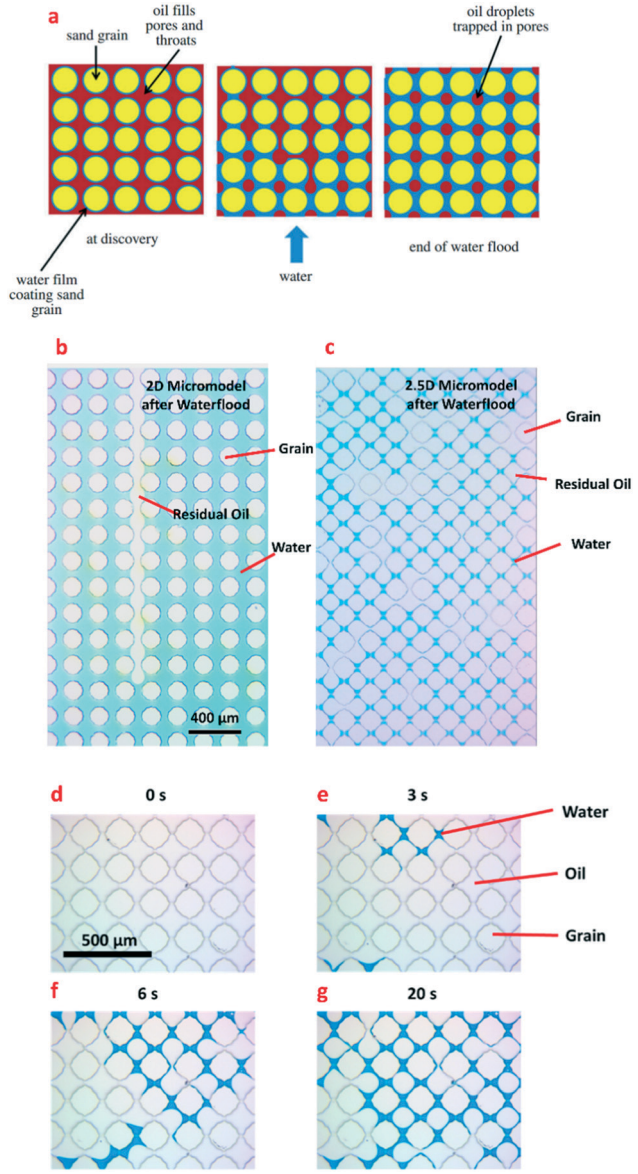

Fig. 2 Validation of 2.5-D micromodel with waterflood experiments. (a) Classical theory on waterflood in water-wet porous media described in ref. 10, where isolated oil droplets could be formed in pores due to capillary snap-off after flooding. (b) Microscopic image of post-waterflood 2-D micromodel, where the pores are either completely occupied by water, or occupied by a continuous oil phase, with no isolated residual oil droplet observed. (c) Microscopic image of post-waterflood 2.5-D micromodel, where most pores are occupied by isolated oil droplets. (d)–(g) Water imbibition into oil-saturated 2.5-D micromodel at different times. It can be observed that the water only flows along the throats and the edges of the channel, without displacing the oil in the pore bodies, and isolated oil droplets are thus trapped in the pore body. The flow direction is from left to right.

which prefer routs with larger curvature when water is the wetting phase. Connections between oil phase in neighbouring pore bodies "snap off" due to the 2.5-D feature at the throats, thus the water phase isolates the oil phase from a continuous phase into dispersed oil droplets trapped in the pore. As a comparison, the waterflood in the 2D micromodel is shown in Movie SB.† In the 2-D case, although the preferential flow of the wetting fluid along the grain edges could also be observed (as in our experiment and by Zhao *et al.*[50]), grain edges are isolated, without efficient connections to conduct water from one grain to the next (which is the role of throats in the 2.5-D micromodel). Thus, snap-off does not happen simultaneously.

In summary, the waterflood experiment on micromodels showed that the 2.5-D geometry successfully introduced necessary 3-D features into the micromodel. Capillary snap-off of oil at the throat, and the formation of isolated trapped oil droplets, were successfully realized on the 2.5-D micromodel, which could not be observed from the 2-D micromodel, neither in previous studies or our own experiments. 2.5-D micromodel is thus promising for research on multi-phase flow in porous media.

Emulsion flooding

Emulsion and foam fluidics in porous media is a growing research area for both enhanced oil recovery and in the chemical/food industry. A long-standing question is how the size of non-wetting phase droplets/bubbles varies spatially in the porous medium. It has been shown that varying the droplet size alone may lead to 10^4 times difference in emulsion apparent viscosity.[51] As explained in the introduction section, capillary snap-off is believed to be the dominant droplet/bubble break-up mechanism but it is very difficult to investigate using a 2-D micromodel.[34] We show that snap-off in emulsion flooding (similar to foam flooding in most aspects) can be easily observed and studied on 2.5-D micromodels. To our knowledge, this is the first published successful emulsion flooding experiment using a micromodel platform.

Octane was used as the oil phase in the experiment, and 1000 ppm silica nanoparticle (5 nm in diameter) and 500 ppm Tween 80 (surfactant) were added into dyed water as emulsion-stabilizer. Oil and aqueous phases are co-injected both at 7 μl h^{-1} flow rate. A video at the inlet demonstrating oil droplet break-up can be viewed in Movie SC,† where different droplet break-up mechanisms can be observed: cut-off by continuous phase's shearing, pinch-off by neighbouring droplets and capillary snap-off.

The microscopic images of emulsion flow at the inlet and 2 cm downstream are shown in Fig. 3a and b. We can observe from those images that the oil phase intensely breaks-up in the very short distance close to the inlet, leading to a rapid decrease in droplet size at this region. However, the droplet size downstream is not much different from that at 1 mm from the inlet. Thus, we can conclude that, in the case that the oil–water interface is well stabilized and the matrix is homogeneous, dispersed phase droplet/bubble size becomes stable at a very short distance from the inlet. The stable droplet size is of the same scale of the throats, as shown in Fig. 3c, indicating that snap-off is the dominant droplet break-up mechanism. The droplet size evolution along the matrix is plotted as shown in Fig. 3d.

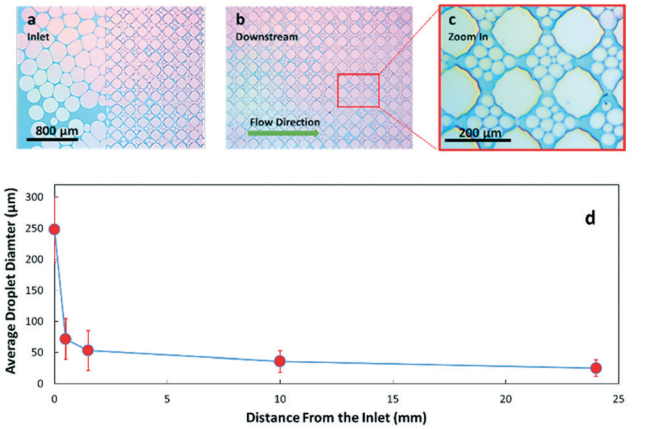

Fig. 3 Emulsion flooding in a 2.5-D micromodel. a) Microscopic image at the inlet of the 2.5-D micromodel. It can be observed that the injected large droplets breakup over very short distances. b) Microscopic image at 2 cm downstream of the inlet, where it can be observed that the droplet size is similar to those close to the inlet after break-up. c) A zoom-in of (b) where we can see that most droplets' size is in similar scale to the throat size. d) Droplet size change along the porous medium, from the beginning to the outlet, with standard deviation marked as the red vertical error bars.

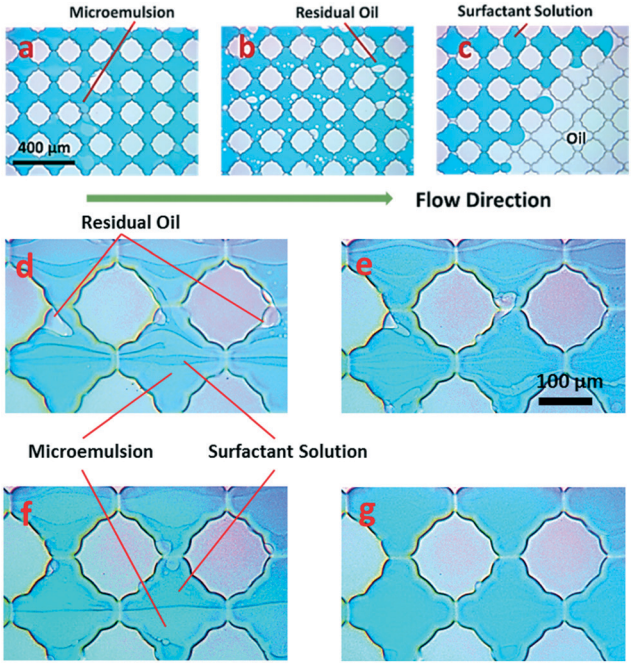

Fig. 4 Surfactant flooding process in 2.5-D micromodel. (a)–(c): Microscopic images of the flooding micromodel from upstream to downstream, where we can visualize a distinct water–oil two phase front at the oil–water contact line in (c), residual oil following the front in (b), and microemulsion phase in far upstream in (a). (d)–(g): Zoom-in images of a fixed region in surfactant flooding with a 4 min time interval to capture. Microemulsion can be observed generated from residual oil in (d) and (e), and then co-flowing with water phase like a belt in (f), and the whole region was finally with neither residual oil nor microemulsion as shown in (g).

Ultra-low IFT surfactant flooding

Enhanced oil recovery by injecting ultra-low IFT surfactants (surfactant flooding) is reported to recover more than 90% of oil in a light-oil reservoir.[52] Among all three types of ultra-low IFT systems (10^{-2}–10^{-4} mN m^{-1}), bi-continuous microemulsion can be generated and is reported to have the best oil displacement efficiency.[52] The fluidic properties and behaviours of the microemulsion phase is an important problem for understanding this process. However, although 2-D micromodels have been applied to study the surfactant flooding process, there are no published studies of a flowing microemulsion phase in a micromodel (although it has been frequently studied by coreflood (real 3-D) experiments[53]). Howe *et al.*[54] recently reported microemulsion phase as a residual phase in a 2-D micromodel, but no evidence about the flowing microemulsion phase was presented.

An ultra-low IFT system, identical to that of Liang,[55] was used to perform a surfactant flooding experiment on our 2.5 D micromodel. The IFT is 8.5×10^{-4} mN m^{-1}, calculated from *Huh Equation*.[56] It is a "Type-III" system, where the microemulsion forms an independent phase rather than dissolved in oil or aqueous phase. The micromodel was pre-saturated with oil, and surfactant solution was then flooded at 15 μl h^{-1}. Microscopic images from upstream to downstream are shown in Fig. 4a–c. A stable water–oil front can be clearly observed, as shown in Fig. 4c, while microemulsion is not observed at the water–oil front.

However, several millimetres behind the front, residual oil droplets can be observed in Fig. 4b, and flowing microemulsion can be observed co-flowing with aqueous phase further upstream, as shown in Fig. 4a. Fig. 4d and e show the process of residual oil (white liquid attached on grains) gradually being dissolved into microemulsion phase (light-blue liquid coming from residual oil which has a clear interface between both aqueous phase and oil phase) and then co-flowing with the aqueous phase (blue liquid). Fig. 4f and g show how the microemulsion phase gradually disappears during the surfactant flooding. Almost all oil, both in oil phase and in microemulsion phase, were finally successfully recovered, as shown in Fig. 4g.

The shifting process from oil phase to microemulsion phase, and the co-flowing of microemulsion phase along with the aqueous phase, which has never been observed on 2-D micromodels, can now be observed. We attribute it to much better ability of 2.5-D micromodel in trapping residual oil due to the more significant and realistic pore-throat geometry: it affects the flow field and generates "dead zones" (low velocity zones) at the pore edges, where oil is more likely to be trapped.

From this experiment, we find two major conclusions relevant to surfactant enhanced oil recovery. 1) There is a microemulsion zone during surfactant flooding, which is upstream of the water–oil front but not closely following the front, which agrees with the observations in coreflood experiments;[53] 2) the microemulsion is generated from the residual oil in the swept region, and then co-flows along with aqueous phase without further trapping. This leads to an almost

100% water region without oil left behind, which agrees with most surfactant EOR coreflood data.[52] We plan further investigation expanding on these novel results.

Conclusions

We developed a novel 2.5-D micromodel fabrication technique on glass microchips, with no more complexity in fabrication than traditional 2-D micromodels. Variation in depth was included in the 2.5-D micromodel in order to better mimic real 3-D porous media. Phenomena that occur in 3-D micron-scale porous media, such as capillary snap-off and formation of isolated residual oil droplet in water-wet media, were successfully realized on 2.5-D micromodel (overcoming 2-D micromodels' inability to capture the physics). The work demonstrates that 2.5-D micromodels could be a more advanced tool to investigate multi-phase flow in porous media.

We observed for the first time a successful oil–water emulsion-flood on a micromodel. The experiment showed that large droplets break into throat-sized smaller droplets in very short distances from the inlet of the porous medium, and then approximately maintain the size constant downstream until the outlet.

In another experiment, ultra-low IFT surfactant was flooded in the 2.5-D micromodel; evaluation of flowing microemulsion phase was observed and described on a micromodel for the first time. The experiment on a 2.5-D micromodel can explain the phenomena observed from experiments on real 3-D, macro-scale porous media.

We gratefully acknowledge support from the sponsors of the Nanoparticles for Subsurface Engineering Industrial Affiliates Project at the University of Texas at Austin.

Notes and references

1 J. Philip, *Flow in porous media, in Theoretical and applied mechanics*, Springer, 1973, pp. 279–294.
2 L. Feng, *et al.*, A super-hydrophobic and super-oleophilic coating mesh film for the separation of oil and water, *Angew. Chem., Int. Ed.*, 2004, **43**(15), 2012–2014.
3 R. Cahn and N. Li, Separation of phenol from waste water by the liquid membrane technique, *Sep. Sci.*, 1974, **9**(6), 505–519.
4 M. Van der Waarden, A. Bridie and W. Groenewoud, Transport of mineral oil components to groundwater—I: Model experiments on the transfer of hydrocarbons from a residual oil zone to trickling water, *Water Res.*, 1971, **5**(5), 213–226.
5 P. A. Gauglitz, *et al.*, Foam generation in homogeneous porous media, *Chem. Eng. Sci.*, 2002, **57**(19), 4037–4052.
6 N. Christov, *et al.*, Capillary mechanisms in membrane emulsification: oil-in-water emulsions stabilized by Tween 20 and milk proteins, *Colloids Surf., A*, 2002, **209**(1), 83–104.
7 R. Gupta, *et al.*, Enhanced Waterflood for Carbonate Reservoirs-Impact of Injection Water Composition, in *SPE Middle East Oil and Gas Show and Conference*, Society of Petroleum Engineers, 2011.
8 D. Tanzil, G. J. Hirasaki and C. A. Miller, Mobility of foam in heterogeneous media: Flow parallel and perpendicular to stratification, in *SPE Annual Technical Conference and Exhibition*, Society of Petroleum Engineers, 2000.
9 M. Auset and A. A. Keller, Pore-scale processes that control dispersion of colloids in saturated porous media, *Water Resour. Res.*, 2004, **40**, W03503.
10 A. Muggeridge, *et al.*, Recovery rates, enhanced oil recovery and technological limits, *Philos. Trans. R. Soc., A*, 2014, **372**(2006), 20120320.
11 M. Sohrabi, *et al.*, A Thorough Investigation of Mechanisms of Enhanced Oil Recovery by Carbonated Water Injection, in *SPE Annual Technical Conference and Exhibition*, Society of Petroleum Engineers, 2015.
12 S. Tavassoli, *et al.*, Low-Salinity Surfactant Flooding—A Multimechanistic Enhanced-Oil-Recovery Method, *SPE J.*, 2015, SPE-173801-PA.
13 G. Cheraghian and L. Hendraningrat, A review on applications of nanotechnology in the enhanced oil recovery part B: effects of nanoparticles on flooding, *Int. Nano Lett.*, 2016, **6**(1), 1–10.
14 H. Gong, *et al.*, Effect of wettability alteration on enhanced heavy oil recovery by alkaline flooding, *Colloids Surf., A*, 2016, **488**, 28–35.
15 D. Cuthiell, *et al.*, Steam corefloods with concurrent X-ray CT imaging, *J. Can. Pet. Technol.*, 1993, **32**(03), PETSOC-93-03-03.
16 P. Qi, *et al.*, Reduction of Residual Oil Saturation in Sandstone Cores using Viscoelastic Polymers, in *SPE Improved Oil Recovery Conference*, Society of Petroleum Engineers, 2016.
17 J.-H. Xu, *et al.*, Extraction performance of a new mixer-settler with membrane dispersion technique, *J. Chem. Eng. Chin. Univ.*, 2003, **17**(4), 361–364.
18 N. S. Gunda, *et al.*, Reservoir-on-a-chip (ROC): a new paradigm in reservoir engineering, *Lab Chip*, 2011, **11**(22), 3785–3792.
19 K. Xu, *et al.*, Microfluidic Investigation of Nanoparticles' Role in Mobilizing Trapped Oil Droplets in Porous Media, *Langmuir*, 2015, **31**(51), 13673–13679.
20 G. L. Morini, Single-phase convective heat transfer in microchannels: a review of experimental results, *Int. J. Therm. Sci.*, 2004, **43**(7), 631–651.
21 G. Romeo, *et al.*, Viscoelastic flow-focusing in microchannels: scaling properties of the particle radial distributions, *Lab Chip*, 2013, **13**(14), 2802–2807.
22 A. Author, Multiphase flow in lab on chip devices: A real tool for the future?, *Lab Chip*, 2008, **8**(7), 1010–1014.
23 A. Günther and K. F. Jensen, Multiphase microfluidics: from flow characteristics to chemical and materials synthesis, *Lab Chip*, 2006, **6**(12), 1487–1503.
24 A. Riaud, *et al.*, A facile pressure drop measurement system and its applications to gas–liquid microflows, *Microfluid. Nanofluid.*, 2013, **15**(5), 715–724.

25 K. Xu, *et al.*, Direct measurement of the differential pressure during drop formation in a co-flow microfluidic device, *Lab Chip*, 2014, **14**(7), 1357–1366.
26 V. van Steijn, C. R. Kleijn and M. T. Kreutzer, Predictive model for the size of bubbles and droplets created in microfluidic T-junctions, *Lab Chip*, 2010, **10**(19), 2513–2518.
27 T. Ward, *et al.*, Microfluidic flow focusing: Drop size and scaling in pressure versus flow-rate-driven pumping, *Electrophoresis*, 2005, **26**(19), 3716–3724.
28 Y.-C. Tan, Y. L. Ho and A. P. Lee, Droplet coalescence by geometrically mediated flow in microfluidic channels, *Microfluid. Nanofluid.*, 2007, **3**(4), 495–499.
29 L. Yang, *et al.*, Experimental study of microbubble coalescence in a T-junction microfluidic device, *Microfluid. Nanofluid.*, 2012, **12**(5), 715–722.
30 P. Mary, V. Studer and P. Tabeling, Microfluidic droplet-based liquid–liquid extraction, *Anal. Chem.*, 2008, **80**(8), 2680–2687.
31 K. Xu, *et al.*, A Microfluidic Investigation of the Synergistic Effect of Nanoparticles and Surfactants in Macro-Emulsion-Based Enhanced Oil Recovery, *SPE J.*, 2016, SPE-179691-PA.
32 V. A. Lifton, Microfluidics: an enabling screening technology for enhanced oil recovery (EOR), *Lab Chip*, 2016, **16**(10), 1777–1796.
33 A. Emadi and M. Sohrabi, Visual investigation of low salinity waterflooding, in *International Symposium of the Society of Core Analysts*, Aberdeen, Scotland, UK, 2012.
34 C. A. Conn, *et al.*, Visualizing oil displacement with foam in a microfluidic device with permeability contrast, *Lab Chip*, 2014, **14**(20), 3968–3977.
35 K. Ma, *et al.*, Visualization of improved sweep with foam in heterogeneous porous media using microfluidics, *Soft Matter*, 2012, **8**(41), 10669.
36 M. Mohajeri, M. Hemmati and A. S. Shekarabi, An experimental study on using a nanosurfactant in an EOR process of heavy oil in a fractured micromodel, *J. Pet. Sci. Eng.*, 2015, **126**, 162–173.
37 J. Herbas, *et al.*, Comprehensive Micromodel Study to Evaluate Polymer EOR in Unconsolidated Sand Reservoirs, in *SPE Middle East Oil & Gas Show and Conference*, Society of Petroleum Engineers, 2015.
38 J. Roof, Snap-off of oil droplets in water-wet pores, *Soc. Pet. Eng. J.*, 1970, **10**(01), 85–90.
39 T. Anderson, Applications of Additive Manufacturing to Rock Analogue Fabrication, in *SPE Annual Technical Conference and Exhibition*, Society of Petroleum Engineers, 2016.
40 A. K. Au, *et al.*, 3D-Printed Microfluidics, *Angew. Chem., Int. Ed.*, 2016, **55**, 3862–3881.
41 A. A. Yazdi, *et al.*, 3D printing: an emerging tool for novel microfluidics and lab-on-a-chip applications, *Microfluid. Nanofluid.*, 2016, **20**(3), 1–18.
42 K. Xu, *et al.*, A region-selective modified capillary microfluidic device for fabricating water–oil Janus droplets and hydrophilic–hydrophobic anisotropic microparticles, *RSC Adv.*, 2015, **5**(58), 46981–46988.
43 G. Takei, *et al.*, Tuning microchannel wettability and fabrication of multiple-step Laplace valves, *Lab Chip*, 2007, **7**(5), 596–602.
44 P. Gravesen, J. Branebjerg and O. S. Jensen, Microfluidics-a review, *J. Micromech. Microeng.*, 1993, **3**(4), 168.
45 M. Buchgraber, *et al.*, Creation of a dual-porosity micromodel for pore-level visualization of multiphase flow, *J. Pet. Sci. Eng.*, 2012, **86–87**, 27–38.
46 L. W. Lake, *Enhanced oil recovery*, 1989.
47 M. Dong and I. Chatzis, The imbibition and flow of a wetting liquid along the corners of a square capillary tube, *J. Colloid Interface Sci.*, 1995, **172**(2), 278–288.
48 L.-C. Chang, *et al.*, Experimental study on imbibition displacement mechanisms of two-phase fluid using micro model, *Environ. Earth Sci.*, 2009, **59**(4), 901–911.
49 H. Lee, S. G. Lee and P. S. Doyle, Photopatterned oil-reservoir micromodels with tailored wetting properties, *Lab Chip*, 2015, **15**(14), 3047–3055.
50 B. Zhao, C. W. MacMinn and R. Juanes, Wettability control on multiphase flow in patterned microfluidics, *Proc. Natl. Acad. Sci. U. S. A.*, 2016, **113**(37), 10251–10256.
51 R. Pal, Effect of droplet size on the rheology of emulsions, *AIChE J.*, 1996, **42**(11), 3181–3190.
52 D. O. Shah, *Improved oil recovery by surfactant and polymer flooding*, Elsevier, 2012.
53 J. Lu and G. A. Pope, Optimization of Gravity-Stable Surfactant Flooding in *SPE Western Regional Meeting*, Society of Petroleum Engineers, 2015.
54 A. M. Howe, *et al.*, Visualising surfactant enhanced oil recovery, *Colloids Surf., A*, 2015, **480**, 449–461.
55 T. Liang, *et al.*, Enhancing Hydrocarbon Permeability After Hydraulic Fracturing: Laboratory Evaluations of Shut-ins and Surfactant Additives, in *SPE Annual Technical Conference and Exhibition*, Society of Petroleum Engineers, 2015.
56 C. Huh, Interfacial tensions and solubilizing ability of a microemulsion phase that coexists with oil and brine, *J. Colloid Interface Sci.*, 1979, **71**(2), 408–426.

